ER vesicles and mitochondria move and communicate at synapses

Sergej L. Mironov* and Natalya Symonchuk

DFG-Center 'Molecular Physiology of the Brain', Department of Neuro- and Sensory Physiology, Georg-August-University, Göttingen, Humboldtallee 23, 37073, Germany

*Author for correspondence (e-mail: smirono@gwdg.de)

Accepted 8 September 2006
Journal of Cell Science 119, 4926-4934 Published by The Company of Biologists 2006
doi:10.1242/jcs.03254

Summary

Endoplasmic reticulum (ER) and mitochondria are multifunctional cell organelles and their involvement in Ca^{2+} handling is important in various neural activities. In the respiratory neurons, we observed ER as continuous reticulum in the soma and as isolated vesicles in dendrites. The vesicles moved bidirectionally with intermittent stops and decreased their velocity near exocytotic sites. ER vesicles and mitochondria that resided in these regions changed lumenal Ca^{2+} and mitochondrial potential in concert with synaptic activity. Ca^{2+} release from ER or mitochondria evoked exocytosis. ER vesicles and mitochondria bidirectionally exchanged Ca^{2+}, the efficacy of which depended on the distance between organelles. Depolarisation-evoked exocytosis had different kinetics, depending on whether functional ER vesicles and mitochondria were present in perisynaptic regions and able to exchange Ca^{2+} or only one organelle type was available. Transfer of Ca^{2+} from ER to mitochondria produced long-lasting elevations of residual Ca^{2+} that increased the duration of exocytosis. In slice preparations, synaptic currents in inspiratory neurons were suppressed after disengagement of ER vesicles and mitochondria, and the activity was potentiated after stimulation of Ca^{2+} exchange between the organelles. We propose that communication between perisynaptic ER vesicles and mitochondria can shape intracellular Ca^{2+} signals and modulate synaptic and integrative neural activities.

Supplementary material available online at
http://jcs.biologists.org/cgi/content/full/119/23/4926/DC1

Key words: Vesicular endoplasmic reticulum, Dynamics and motility, Mitochondria, Ca^{2+} signalling, Synaptic activity, Respiratory neurons

Introduction

Mitochondria and endoplasmic reticulum (ER) are important modulators of the signalling pathways that involve intracellular Ca^{2+} ($[Ca^{2+}]_i$). In comparison with non-neuronal cells, where the role of the organelles in sensing and exchanging Ca^{2+} is well documented (Arnaudeau et al., 2001; Berridge, 2002; Rizzuto et al., 2004), the significance of interactions between ER and mitochondria in shaping synaptic and dendritic $[Ca^{2+}]_i$ transients in neurons remains speculative. ER and mitochondria form networks that expand throughout the cell (Terasaki et al., 1994; Spacek and Harris, 1997; Waterman-Storer and Salmon, 1998; Baumann and Walz, 2001; Collins et al., 2002). ER exists both in the form of continuous structure (Spacek and Harris, 1997; Berridge, 2002) and as a mobile vesicular compartment (Bannai et al., 2004). As mitochondria are also mobile, the distribution patterns of both organelles might be influenced by the needs of neurons to optimise the Ca^{2+} handling according to the requirements that can be imposed by neuronal activity and plasticity.

Electron microscopy shows heterogeneous Ca^{2+} sequestration within ER and mitochondria in the dendrites of hippocampal neurons (Pivovarova et al., 2002) and pharmacological exclusion of ER or mitochondria from Ca^{2+} buffering modifies synaptic potentials (Markram et al., 1995; Billups and Forsythe, 2002; Medler and Gleason, 2002; Belair et al., 2005). It remains unclear, however, whether and how the neuronal activity is dependent on the spatiotemporal distribution of ER and mitochondria and which role the interactions between the organelles might play. Even in one cell these interactions might vary, as demonstrated by different properties of the isolated synaptic and non-synaptical cortical mitochondria (Brown et al., 2006).

Here we examined the correlations between synaptic activity in the respiratory neurons and distribution and function of ER and mitochondria as internal Ca^{2+} stores. These cells provide an interesting subject for the study of such relationships because the respiratory neurons are permanently active and exhibit rhythmic depolarisations that are accompanied by cyclic changes in $[Ca^{2+}]_i$ (Koshiya and Smith, 1999; Mironov and Langohr, 2005) and in mitochondrial variables such as NADH, FAD, potential and $[Ca^{2+}]$ (Mironov and Richter, 2001; Mironov et al., 2005a). In the respiratory neurons, the distribution of mitochondria is controlled by the synaptic activity (Mironov, 2006) and these organelles often colocalise with ER that requires intact microtubules (Mironov et al., 2005b). We identified a vesicular ER compartment, showed its functional uncoupling from reticular structures and demonstrated its operation as a local Ca^{2+} store. ER vesicles moved and slowed down in the vicinity of active synapses where they often established long-lasting contacts with mitochondria. Both perisynaptic organelles responded with changes in functional variables (lumenal $[Ca^{2+}]$ and mitochondrial potential) in concert with synaptic activity. The time-course of depolarisation-evoked exocytosis depended on

the presence of functional ER vesicles and mitochondria and on the interactions between the organelles. Enhancement of Ca^{2+} exchange between ER and mitochondria potentiated depolarisation-evoked exocytosis in vitro and respiratory motor output in vivo. Disruption of contacts between the organelles decreased the amplitude and the duration of exocytosis and abolished the respiratory activity. We propose that the presence of ER vesicles and mitochondria in the functional 'hot spots' and their interplay through Ca^{2+} exchange can be important in shaping synaptic activity and in the modulation of the integrative neural activity.

Results

In neurons stained with Mag-Fura-2, the ER had reticular structure in the soma and dot-like formations in dendrites. To verify that Mag-Fura-2 reports intracellular ER distribution, we used neurons that were transfected with enhanced yellow fluorescent protein (EYFP)-calreticulin and loaded them with the dye. The images of Mag-Fura-2 and calreticulin showed an overlap (Fig. 1A). When calreticulin-transfected neurons were stained with ER-Tracker (Molecular Probes) (Mironov et al., 2005b), we measured a similar overlap between corresponding images in five neurons. However, the Tracker cannot be used in combination with Mag-Fura-2 because both dyes have similar excitation and emission spectra. Calreticulin can potentially alter the functional Ca^{2+}-binding within ER, and in all further experiments only Mag-Fura-2 was used. All Mag-Fura-2-stained organelles released Ca^{2+} after addition of sarco-endoplasmic reticulum Ca^{2+}-ATPase (SERCA)-inhibitor thapsigargin to the bath. Local applications of thapsigargin to the soma and to the dendrites produced independent decreases in lumenal [Ca^{2+}] in either compartment (Fig. 1B), indicating that the vesicles and reticulum in the respiratory neurons were functionally uncoupled, which is in line with the data obtained in the hippocampal neurons (Bannai et al., 2004).

In Mag-Fura-2-stained neurons, we counted 232±25 single ER vesicles per cell and the mean distance between them in dendrites was 4.4±1.2 μm. Cross-sections of ER vesicles ranged from 0.7 to 1.4 μm (1.13±0.15 μm, n=77). ER vesicles changed their positions during the experiments (supplementary material Movie 1). The motility of vesicles was first assessed from their dwell areas. They were measured by using a Metamorph routine that reports the maximal values of pixels in consequent frames (Fig. 2A). During a 20-minute-long recording, the positions of particles' centers covered the mean area of 9.8±1.1 μm^2 (n=28 in five cells). Taking this value as a mean square displacement ($<x>^2$) and using the Einstein-Smoluchowski equation $<x>^2=4Dt$ (Saxton and Jacobson, 1997), we obtained the apparent diffusion coefficient of 10 $\mu m^2/4\times1200$ seconds=2×10^{-3} μm^2/second.

For further analysis of ER movements, we applied a single particle tracking (SPT) method (Saxton and Jacobson, 1997; Mironov, 2006). Fig. 2D demonstrates the trajectories of the vesicles and Fig. 2E depicts them as kymographs. The traces show that the vesicles often stopped the movements, 'wiggled' and started to move in either direction. Distribution of velocities (Fig. 2F) were well fitted with a sum of three Gaussian curves, which peaks at 0, 0.2 μm/second and –0.3 μm/second corresponding with the stochastic motion (SM), the anterograde transport (AT) and retrograde transport (RT). The data agree with the values that were determined from the slopes of the kymographs (exemplified in the last trace in Fig. 2F). Their means were 0.25±0.05 μm/second (AT, n=12) and 0.32±0.06 μm/second (RT, n=12 in five cells), respectively. From SPT trajectories we also measured the mean run-times and run-lengths in these three basic movement modes which

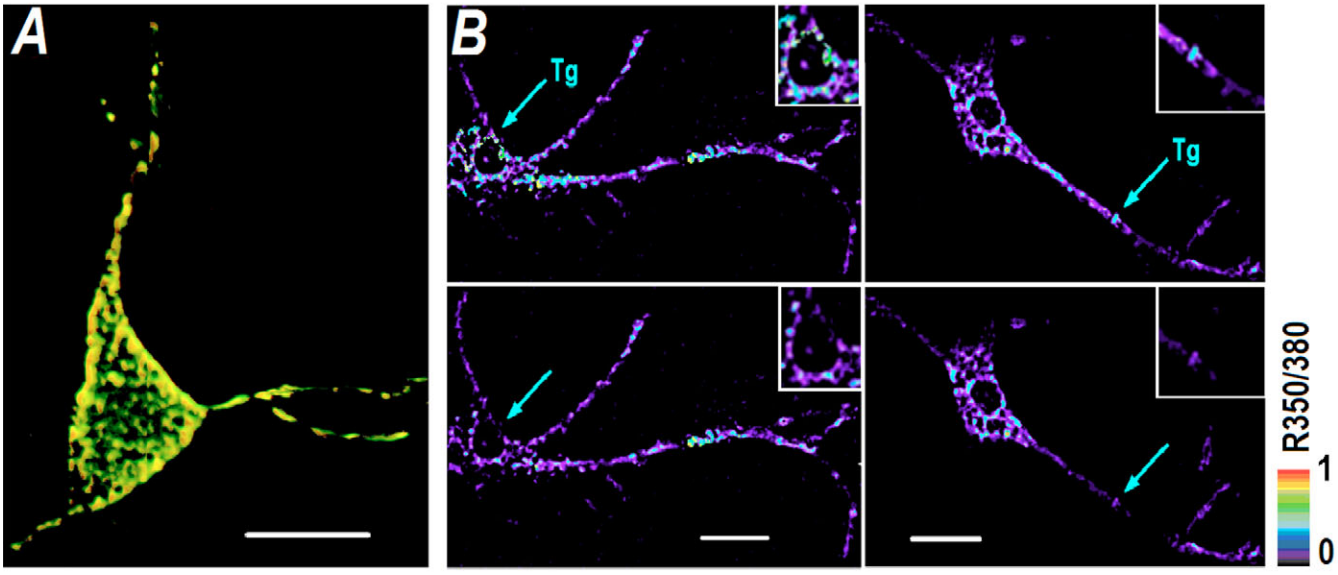

Fig. 1. Identification and continuity of ER in the respiratory neurons. (A) EYFP-calreticulin-transfected and Mag-Fura-2-stained neuron. Fluorescence images of Mag-Fura-2 and EYFP-calreticulin were coded by red and green, respectively, and were merged with yellow pixels indicating an overlap (42% in this image, mean 44±5% in seven cells). (B) Independent decreases in lumenal Ca^{2+} in the soma and in the dendrite after the local application of thapsigargin (Tg, 1 μM). Shown are ratioed images of Mag-Fura-2 fluorescence (350 or 380 nm excitation) measured before (top two panels) and 2 minutes after thapsigargin (lower two panels). Changes at application sites are 2×-enlarged in the right upper-corner of each panel. The arrows indicate the positioning of the application pipette. Similar responses were measured in four other neurons. Bar, 10 μm.

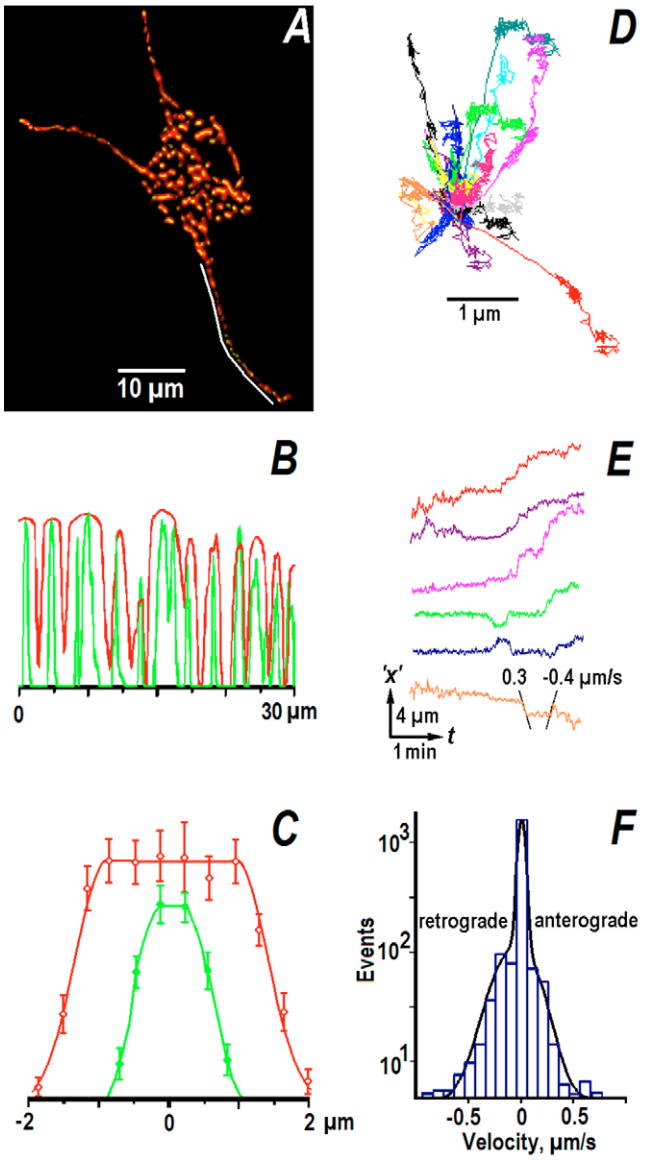

Fig. 2. Motility of ER vesicles. (A) Red image shows the dwell areas of ER vesicles that were obtained as maximal values in a stack of 300 images in the Mag-Fura-2-stained neurons. A green-coded image shows the first frame and indicates initial positions of the vesicles (in the overlay all green pixels are yellow). (B) Fluorescence scans in the dendrite taken along the white line in A. The red and green traces show the dwell areas and positions of the vesicles, respectively. (C) Mean profiles across the vesicles and their dwell areas obtained by averaging linescans for 17 vesicles in dendrites. (D) Trajectories of ER vesicles in one representative dendrite. The traces were repositioned for presentation to begin in one point. Note the episodes of 'wiggling' (small irregular displacements by <0.2 µm) and transportation events. (E) Kymographs of ER vesicles in the *'x'-t* plane where *'x'* corresponds to the one-dimensional curvilinear path in the dendrite. The colours of traces are the same as used in presenting the trajectories in D. Horizontal episodes correspond to the 'wiggling' of the vesicles and inclined displacements represent the episodes of directed transport where velocity is given by the slope of kymographs as exemplified in the last trace. (F) Instantaneous velocities of ER vesicles and their approximation by the sum of three Gaussian curves.

were equal respectively to 7.5±1.7 seconds (SM), 8.4±2.1 seconds (AT) and 8.3±2.3 seconds (RT) and 0.2±0.1 µm (SM), 2.1±0.8 µm (AT) and –3.4±2.1 µm (RT). The pair ratios correspond to the velocities of 0.03 µm/second (SM), 0.25 µm/second (AT) and –0.41 µm/second (RT), which are close to the mean instantaneous velocities (Fig. 2F) and the kymograph slopes.

Mag-Fura-2-stained-ER vesicles and mitochondria that were stained by tetramethylrhodamineethylester (TMRE) showed colocalisation (Fig. 3C). This was frequently observed in the proximity of synapses that were stained by FM 1-43 (Fig. 3). Mean distances between the maxima of the overlapping spots were 0.82±0.14 µm (Mag-Fura-2 versus FM 1-43, n=14), 0.91±0.12 µm (TMRE versus FM 1-43, n=12), and 0.94±0.15 µm (Mag-Fura-2 versus TMRE, n=15), respectively.

Various physiological stimuli changed lumenal [Ca^{2+}] and mitochondrial potential ($\Delta\psi$) in the perisynaptic ER vesicles and mitochondria (Fig. 4). Brief membrane depolarisation triggered exocytosis (indicated by decreases in the FM 1-43 fluorescence) that was accompanied by the transient elevation of ER lumenal Ca^{2+} ($[Ca^{2+}]_{ER}$) (Fig. 4A). During hypoxia, Ca^{2+} was released from ER that also evoked exocytosis (Fig. 4B). This resembled the effects of hypoxia in vivo, which mobilises Ca^{2+} from ER and transiently augments synaptic activity (Mironov and Langohr, 2005). When metabotropic glutamate receptors were activated with trans-1-aminocyclopentane-1,3-dicarboxylic acid (t-ACPD, 100 µM), several releases of Ca^{2+} from ER were observed, each accompanied by exocytosis (Fig. 4C). High-K^+, hypoxia and kainate also induced long-lasting decreases in TMRE fluorescence (Fig. 4D-F, respectively) indicating depolarisation of perisynaptic mitochondria.

ER vesicles and mitochondria both increased their Ca^{2+} content after brief membrane depolarisations (Fig. 5A). Other stimuli induced redistribution of Ca^{2+} between the organelles. For example, when Ca^{2+} was mobilised from ER by applying hypoxia (Fig. 5B), *t*-ACPD (Fig. 5C) and thapsigargin (Fig. 5D), it was taken up by mitochondria. When mitochondria became 'leaky' after their uncoupling with carbonyl cyanide 3-chlorophenylhydrazone (CCCP 1 µM), $[Ca^{2+}]_{ER}$ slowly increased (Fig. 5E). Application of taxol (paclitaxel), which triggers a formation of mitochondrial permeability transition pore (mPTP) in the low-conductance state (Evtodienko et al., 1996; Carre et al., 2002; Kidd et al., 2002; Mironov et al., 2005b), induced Ca^{2+} leak from mitochondria that was accompanied by several releases of Ca^{2+} from neighbouring ER vesicles (Fig. 5F).

Ca^{2+} exchange between ER vesicles and mitochondria demonstrated clear dependence on the distance between the organelles. Fig. 6A shows that Ca^{2+} release from the CCCP-uncoupled mitochondria increased $[Ca^{2+}]_{ER}$ only when the organelles were in a close apposition. The resting Ca^{2+} content was also bigger in the ER vesicles that were located closer to mitochondria. Fig. 6B shows that thapsigargin-induced Ca^{2+} mobilisation from ER was sensed only by those mitochondria that were separated from ER by less than 1 µm.

When mobile mitochondria and ER vesicles approached each other, they often stopped their movements (Fig. 6C, supplementary material Movie 2). This frequently occurred close to exocytotic sites (approximately two-thirds of all events observed). At distances >1 µm between the particles, the

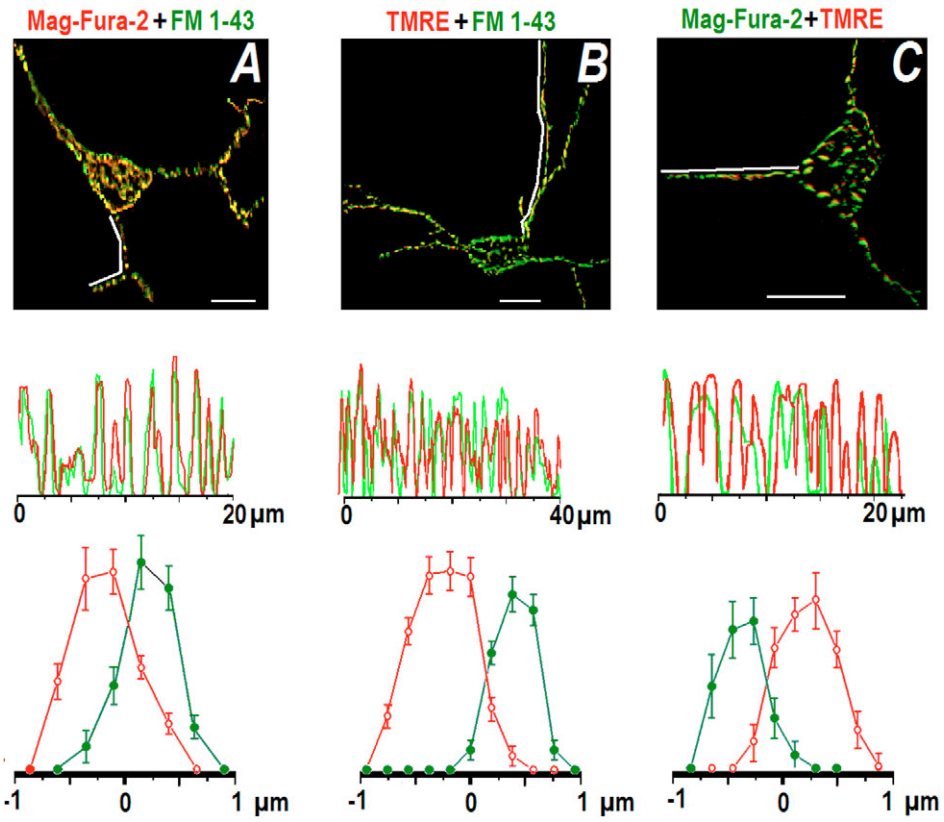

Fig. 3. ER, mitochondria and synaptic vesicles. (A) Colocalisation of ER and synaptic vesicles. The uppermost panel shows the merged images of Mag-Fura-2 (red) and FM 1-43 (green). The overlap between images was 25% (mean 27±6% in six cells). The middle panel presents the fluorescence profiles in the dendrite which indicate positions of ER vesicles (red) and synapses (green). The lowermost panel shows the mean profiles obtained by averaging the data in 15 ROIs that contained both ER and synaptic vesicles. (B) Mitochondria and synaptic vesicles. The uppermost panel shows the images of TMRE (red) and FM 1-43 fluorescence (green). In this image, the coincidence of pixels that corresponded to the positions of mitochondria and synapses was 24% (mean 27±5% in seven cells). The lower graphs show the linescans in dendrites and corresponding mean profiles obtained from 18 ROIs where the positions of synaptic vesicles overlapped with those of mitochondria. (C) Colocalisation of mitochondria and ER vesicles presented as an overlay of Mag-Fura-2 (green) and TMRE images (red). The overlap between positions of ER vesicles and mitochondria in this neuron was 34% (mean 37±6% in seven cells). The middle and the lowermost graphs show respectively the linescans along dendrites and the mean profiles that were obtained by averaging the data for 16 pairs of particles. Bar in all upper panels, 10 µm.

movements shared no interference (occasional pauses such as that in Fig. 6C represent simple interruptions in the directed transport) (Fig. 2D,E). Microtubules are necessary both for the transport (Bannai et al., 2004) and the maintenance of contacts between ER and mitochondria (Mironov et al., 2005b). Here we found that after disruption of microtubules with 5 µM nocodazole (tested in five cells from five different preparations), more than 90% of contacts between the organelles disappeared and after this the movements of vesicles and mitochondria showed no correlation. Nocodazole and taxol, which act on microtubules, might elicit other actions, but in the respiratory neurons we did not observe any effect of these drugs on different voltage-dependent and ligand-regulated channels (reviewed by Richter et al., 2000). The actions of drugs on the exocytotic machinery are also unlikely, because only actin filaments but not microtubules contact with synaptic vesicles (Shupliakov et al., 2002).

We next attempted to reveal possible functional significance of interactions between the ER vesicles and mitochondria. We evoked exocytosis by locally applying the high-K^+ (45 mM) solution to the neural processes. Figs 7 and 8 present the kinetics of exocytosis that were measured as the derivative of the relative FM 1-43 fluorescence, $-d(\Delta F/F_o)/dt$. The time-course of depolarisation-induced exocytosis and accompanying changes in $[Ca^{2+}]_{ER}$ and mitochondrial Ca^{2+} ($[Ca^{2+}]_m$) clearly depended on the presence, positioning and functionality of ER and mitochondria. In the control (Fig. 7A), the rate of exocytosis promptly reached the peak and then decayed bi-exponentially with the time-constants τ=1.2±0.3 seconds and 4.2±1.2 seconds (n=7) which had roughly equal weights. In three other experiments, membrane depolarisation induced several Ca^{2+} releases from ER, each followed by exocytosis (Fig. 7B), reminiscent of the effects of taxol (Fig. 5F). This indicates that the opening of a low-conductance mPTP (Ichas and Mazat, 1998) can also occur at physiological conditions. Fig. 7C shows that when only ER vesicles were present, the increases in $[Ca^{2+}]_{ER}$ were bigger (170±15% of control, P<0.01, n=7) and the decay was monoexponential (τ=1.1±0.2 seconds, n=8). When only mitochondria were present (Fig. 7D), the exocytosis peak slightly increased (115±7% of control, P<0.08, n=8) and the decay was similar (τ=1.0±0.3 seconds, n=7). In five cells pretreated with either thapsigargin or CCCP to deplete ER and mitochondrial Ca^{2+}, respectively, the peaks of exocytosis were equal to 152±14% (P<0.01) and 120±12% (P<0.08), respectively, of mean values measured before the treatment, and the decay time-constants were 1.2±0.1 seconds and 1.1±0.1 seconds. The changes in $[Ca^{2+}]_{ER}$ or $[Ca^{2+}]_m$ (Fig. 7E,F) resembled those measured when only one active organelle was present (Fig. 7C,D).

We also attempted to modulate communication between ER vesicles and mitochondria. When the organelles were disengaged after nocodazole treatment, the peak exocytosis was 63±8% of that measured before the treatment (five trials in five cells from different batches). The changes in $[Ca^{2+}]_{ER}$ were bigger and lasted longer, whereas changes in $[Ca^{2+}]_m$ became smaller and shorter. The transients resembled those recorded in the presence of isolated ER vesicles and mitochondria (Fig. 7C,D). In the presence of taxol, which

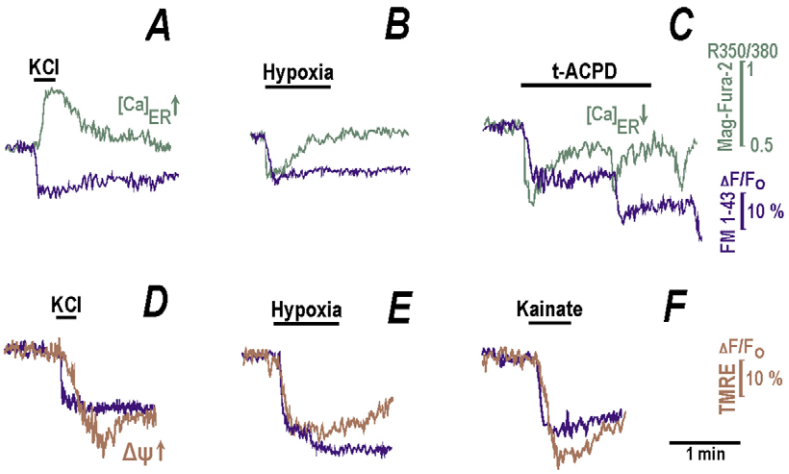

Fig. 4. Synaptic activity, lumenal $[Ca^{2+}]$ and mitochondrial potential. Neurons were stained with FM 1-43 and either Mag-Fura-2 (A-C) or TMRE (D-F). The representative traces (⩾5 pairs collected in ⩾4 neurons) were obtained from the signals measured in the overlapping spots of FM 1-43 and either Mag-Fura-2 or TMRE fluorescence. Changes in $[Ca^{2+}]_{ER}$ are presented as ratios of Mag-Fura-2 signals at 350 or 380 nm. Decreases in TMRE fluorescence indicate mitochondrial depolarisations. Note that all applied stimuli, 45 mM KCl (A,D), hypoxia (B,E), 100 μM t-ACPD (C), and 1 μM kainate (F) decreased the fluorescence of FM 1-43, indicating exocytosis.

stimulates Ca^{2+} efflux from mitochondria (see above), the peak of exocytosis increased to 149±15% and its time-course was significantly prolonged (Fig. 8D, the two time-constants were equal to 2.2±1.2 seconds and 6.2±1.1 seconds, n=6). In taxol, $[Ca^{2+}]_{ER}$ changes lasted longer, whereas $[Ca^{2+}]_m$ transients were smaller and shorter.

Finally, we tested the role of interactions between mitochondria and ER in the integrative activity of the respiratory network. For this, we used a functional slice preparation (Smith et al., 1991; Mironov et al., 1998) and the whole-cell recordings in the perforated patch mode. In this functional isolated respiratory network, the inspiratory neurons show spontaneous synaptic currents that are grouped into synaptic drives discharging synchronously with the respiratory motor output (Smith et al., 1991). Two minutes after addition of thapsigargin or CCCP to the slice, the spontaneous synaptic currents were suppressed and synaptic drives disappeared (n=4 for each drug, data not shown). When the contacts between ER and mitochondria were modified by the microtubule-acting drugs, both the synaptic activity and the respiratory motor output in vivo were changed: nocodazole abolished both synaptic drives and the respiratory motor output, and taxol produced a long-lasting potentiation of these activities (Fig. 9).

Discussion

In many respects the proper functioning of neurons depends on their ability to form and maintain synapses, the operation of which is required in various neuronal activities. The synapses that are frequently activated should receive adequate energy supply and properly handle elevations of $[Ca^{2+}]_i$. The presence of mitochondria (Stowers et al., 2002; Guo et al., 2005; Verstreken et al., 2005) and ER in the proximity of synapses can be crucial for maintaining the synaptic activity in neurons. ER and mitochondria are involved in the modulation of synaptic transmission (Markram et al., 1995; Billups and Forsythe, 2002; Medler and Gleason, 2002; Belair et al., 2005). The disturbances in $[Ca^{2+}]_i$ handling by these organelles can cause necrosis and apoptosis (White et al., 2005). ER and mitochondria often participate in different forms of short- and long-term plasticity (Reyes and Stanton, 1996; Takechi et al., 1998; Takei et al., 1998; Miyata et al., 2000). In non-neuronal cells, mitochondria often exchange Ca^{2+} with the neighbouring ER (Arnaudeau et al., 2001; Malli et al., 2003; Rizzuto et al., 2004). Whether such interactions occur in neurons and how they are related to neuronal activity is unknown.

Mitochondria are mobile and can relocate (Bereiter-Hahn and Voth, 1994), slowing down in the proximity of synapses (Mironov, 2006). ER is often considered as a fixed continuous structure (Spacek and Harris, 1997; Berridge, 2002) but the electron microscopy of Purkinje neurons (Volpe et al., 1991) and imaging of the living hippocampal neurons (Bannai et al., 2004) indicate that ER can also exist in the form of an isolated vesicular compartment that is mobile. When such ER vesicles can store Ca^{2+} and exchange it with mitochondria, this raises a possibility of complex spatiotemporal interactions between the organelles (Rizzuto et al., 2004).

We documented the presence of vesicular ER structures in the processes of respiratory neurons where they functioned as local Ca^{2+} stores. During exocytosis, the lumenal $[Ca^{2+}]$ in ER vesicles was transiently elevated and release of Ca^{2+} from ER triggered exocytosis. ER vesicles moved bidirectionally with intermittent stops (Fig. 2) that had much in common with the motility of mitochondria (Bereiter-Hahn and Voth, 1994). When ER vesicles and mitochondria approached each other in perisynaptic areas, both organelles slowed down their movements (Fig. 6, supplementary material Movies 1 and 2). This can be because of steric hindrance or involve $[Ca^{2+}]_i$, the levels of which can be elevated in the interstitial space and suppress the movements of particles (Yi et al., 2004; Brough et al., 2005). The perisynaptic ER vesicles and mitochondria exchanged Ca^{2+} in both directions (from mitochondria to ER and backwards) and this occurred after applications of various neurotransmitters and during hypoxia (Fig. 5).

Exocytosis induced by local membrane depolarisations showed a clear dependence on the presence of functional ER vesicles or mitochondria (Fig. 7) and the efficacy of the exchange of Ca^{2+} between the organelles (Fig. 6). The time-course of the depolarisation-induced exocytosis was shorter when one organelle was absent or not functional after the Ca^{2+} uptake into the organelles was impaired. In these cases, the changes in $[Ca^{2+}]_{ER}$ and $[Ca^{2+}]_m$ were also different. When mitochondria were absent or non-functional, the maximal rate of exocytosis increased but its duration shortened. $[Ca^{2+}]_{ER}$ transients were bigger and lasted longer than in the control (Fig. 7C,E). Without functional ER vesicles, exocytosis was shorter in duration and the $[Ca^{2+}]_m$ transients were smaller (Fig. 7D,F).

Exocytosis was also dependent on the efficacy of the exchange of Ca^{2+} between the organelles (Fig. 6). When one

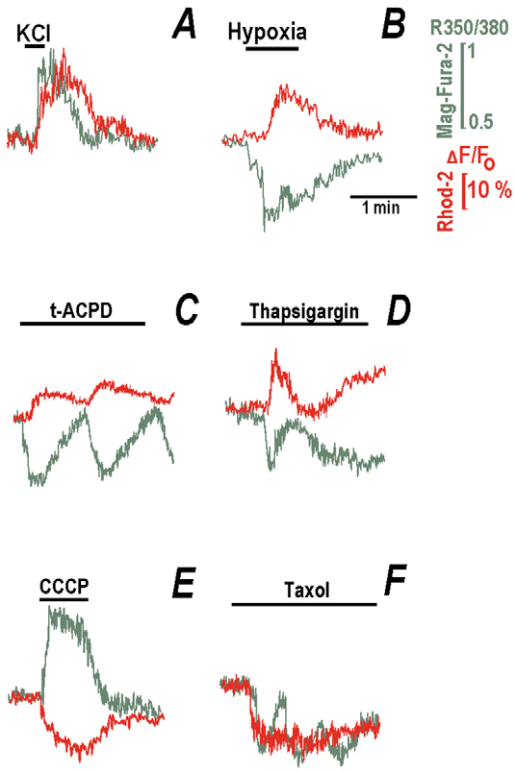

Fig. 5. Ca^{2+} exchange between mitochondria and ER. ER vesicles and mitochondria were labelled with Mag-Fura-2 and Rhod-2, respectively. KCl (45 mM) (A), hypoxia (B), 100 μM *t*-ACPD (C), 1 μM thapsigargin (D), 1 μM CCCP (E) and 3 μM Taxol (F) were applied as indicated. The traces were obtained from fluorescence changes in the areas that contained both ER vesicles and mitochondria. The data are representative of at least five trials for each protocol performed in neurons from three different cell batches.

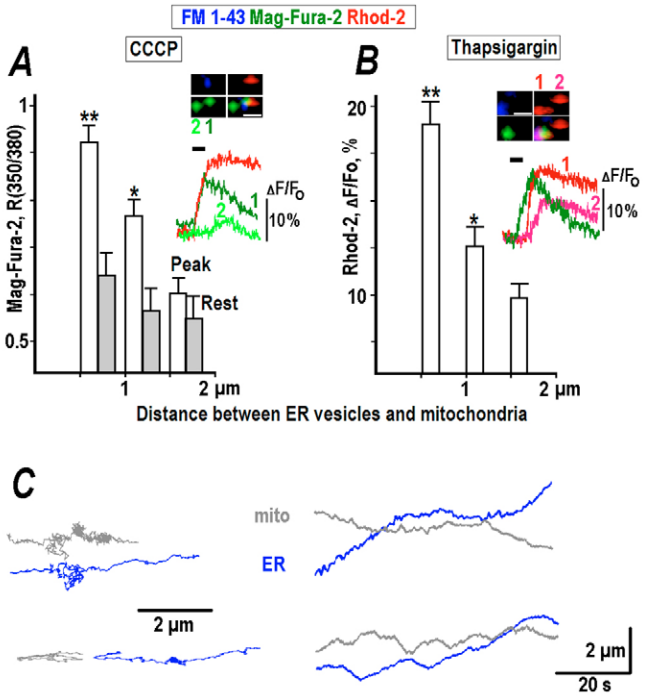

Fig. 6. Spatiotemporal interactions between mitochondria and ER. (A) Mean Mag-Fura-2 signals in ER vesicles measured during Ca^{2+} release from mitochondria because of 1 μM CCCP versus separation of ER vesicles and mitochondria. Peak (open bars) and resting ratios (grey bars) of fluorescence at 350 nm/380 nm were cumulated into the 0.5 μm-wide bins (n>7 for each), averaged and plotted as histograms where the vertical bars show standard deviations. The asterisks indicate the significance (**P<0.01; *P<0.05). Exocytotic sites were locally depolarised with 45 mM KCl and representative measurements are demonstrated in the inset where the four small panels show ROIs with blue-, green- and red-coded images representing corresponding images of FM 1-43, Mag-Fura-2 and Rhod-2, and their overlay (Bar, 1.5 μm). Red and green curves show the relative changes in Mag-Fura-2 and Rhod-2 fluorescence which was measured in single organelles as indicated near the frames. (B) The dependence of relative peak changes in Rhod-2 fluorescence because of 1 μM thapsigargin on the distance between ER vesicles and mitochondria. The coding of frames in B is similar to that in A. (C) Interference between the movements of mitochondria and ER vesicles. The left panel shows two typical trajectories of ER vesicles and mitochondria in dendrites that are also presented as kymographs in the right panel. Note a bilateral suppression of movements of mitochondria and ER vesicles upon their approach as shown by the couple of traces in the upper panel that are representative for 33 stops of mitochondria by ER vesicles and 11 stops of ER vesicles by mitochondria analysed in 27 cells. The lowermost part of the figure shows the absence of correlation between the movements of organelles that did not come close (the occasional pauses in movements here were caused by interruptions of the directed transport of organelles).

organelle was absent or not functional after the impairment of Ca^{2+} uptake and concomitant leakage of Ca^{2+} out of the lumen, the time-course of exocytosis shortened. When mitochondria were absent or non-functional, the exocytosis peak increased and $[Ca^{2+}]_{ER}$ elevations were bigger and lasted longer than in the control (Fig. 7C,E). Without functional ER vesicles, the maximal rate of exocytosis increased only slightly, and the $[Ca^{2+}]_m$ transients were smaller and shorter (Fig. 7D,F).

These observations cannot be explained by assuming independent contributions of ER and mitochondria to the Ca^{2+} buffering. Accumulations of Ca^{2+} in ER and mitochondria were always transient (Figs 4-8) and the organelles slowly returned Ca^{2+} back into the cytoplasm. After exclusion of mitochondria from Ca^{2+} buffering, $[Ca^{2+}]_{ER}$ transients became larger (Fig. 7C), indicating that some Ca^{2+} is normally transferred from ER to the neighbouring mitochondria. The resulting local elevations of $[Ca^{2+}]_i$ can prolong exocytosis via a 'residual Ca^{2+} mechanism' (Zucker, 1999), leading to potentiation of synaptic potentials. We also expect similar long-term $[Ca^{2+}]_i$ elevations because of the interactions between ER and mitochondria at postsynaptic sites where they can modulate the signalling pathways involved in the long-term potentiation of synaptic transmission (Kampa et al., 2006).

We believe that communication between ER and mitochondria contributes to the electrical activity in persistently active neurons. Our data indicate that when perisynaptic ER vesicles and mitochondria were disengaged after disruption of microtubules with nocodazole, the uptake of Ca^{2+} by ER and mitochondria proceeded independently and the peak and duration of exocytosis was reduced. Taxol induces $[Ca^{2+}]_i$ spikes and waves in secretory cells (Kidd et al., 2002) and in the respiratory neurons (Mironov et al., 2005b). Cyclic $[Ca^{2+}]_i$ changes are evident during the respiratory activity

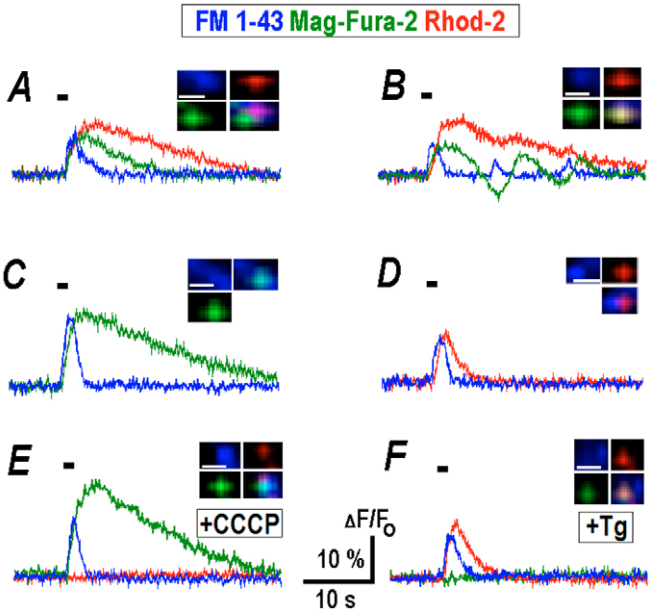

Fig. 7. Modulation of exocytosis by mitochondria and ER vesicles. Synaptic vesicles, ER and mitochondria stained with FM 1-43, Mag-Fura-2 or Rhod-2. The ROIs are shown in the insets by blue-, green- and red-coded images, respectively (Bars, 1 μm). Synaptic activity was induced by locally applying high-K^+ solutions as indicated by the horizontal bars. The application pipette was positioned 2 μm from the spots of FM 1-43 fluorescence. The time-course of exocytosis was measured as a derivative of the relative FM 1-43 fluorescence, $-d(\Delta F/F_o)/dt$. Shown are representative experiments (⩾5 trials for each protocol) performed in neural processes at sites that contained ER vesicles and mitochondria (A,B,E,F), only ER vesicles (C) and only mitochondria (D). Note two additional peaks in B that corresponded to spontaneous Ca^{2+} releases from ER, each accompanied by exocytosis. In the experiment shown in E, 1 μM CCCP was first applied to the bath for 2 minutes and then exocytosis was locally evoked. In F, 1 μM thapsigargin was first applied to the bath for 2 minutes and then a local membrane depolarisation was applied. Note also a weaker fluorescence of Mag-Fura-2 (excited at 350 nm) and Rhod-2 after the inhibition of Ca^{2+} uptake into the corresponding organelle.

(Koshiya and Smith, 1999) which also involves ER and mitochondria (Mironov and Langohr, 2005). In HeLa cells (Ishii et al., 2006), the Ca^{2+} shuttling between the organelles modulates the $[Ca^{2+}]_i$ oscillations. The rhythmic discharges in the inspiratory neurons are driven by the barrages of synaptic potentials ('synaptic drives'), which are modulated by $[Ca^{2+}]_i$ (Mironov and Langohr, 2005). When exocytosis is prolonged, a summation of synaptic potentials will produce a bigger output. As a result, the membrane potential at the soma will cross a threshold for the burst generation and a neuron will be depolarised for a longer time period. When exocytosis shortens, only a few brief synaptic potentials will be generated and their cumulative action might not be sufficient to trigger the bursting activity. Here we observed a suppression of the respiratory motor output after disruption of contacts between ER and mitochondria in vivo, and potentiation of the rhythmic activity after enhancement of the Ca^{2+} exchange between the organelles with taxol (Fig. 8). This prompts speculation that similar interactions between ER and mitochondria can

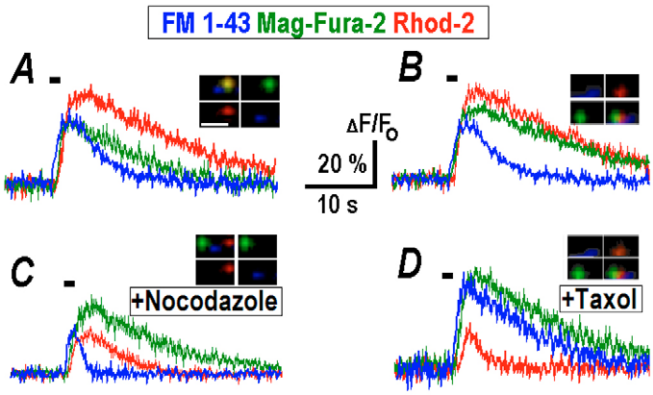

Fig. 8. Changes in exocytosis because of communication between mitochondria and ER vesicles. Synaptic vesicles, ER and mitochondria stained with FM 1-43, Mag-Fura-2 or Rhod-2. The ROIs are shown in the insets by blue-, green- and red-coded images, respectively (Bar, 1 μm). Exocytosis was induced by local applications of high-K^+ solutions as indicated by the horizontal bars and its time-course was measured as the derivative of relative FM 1-43 fluorescence, $-d(\Delta F/F_o)/dt$. Shown are representative experiments performed at synaptic sites that contained both ER vesicles and mitochondria in the control (A,B) and 5 minutes after addition of 5 μM nocodazole (C) and 0.1 μM taxol (D) to the bath. Note separation of the initially contacting ER vesicles and mitochondria after nocodazole, the shortening of exocytosis in the presence of nocodazole and its prolongation by taxol.

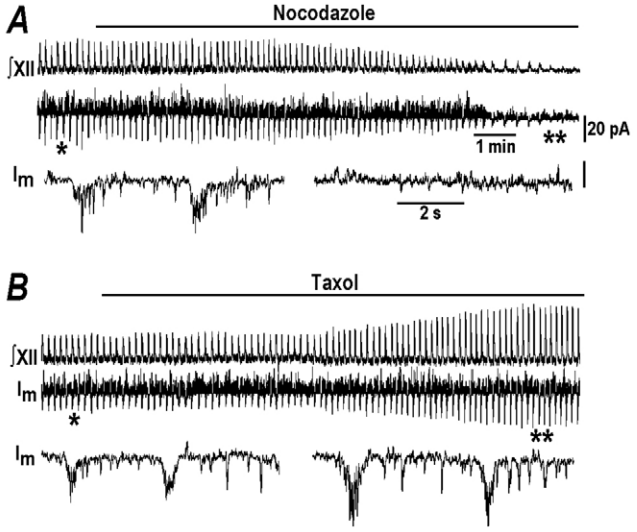

Fig. 9. Modulation of the respiratory motor output in vivo after modification of contacts between ER and mitochondria. Shown are the effects of 5 μM nocodazole (A) and 0.1 μM taxol (B). The two traces in each panel present the respiratory motor output (∫XII) and the membrane current (I_m) recorded at the holding potential of –40 mV. The episodes marked by asterisks are expanded in the lower part of each panel. Note differential effects of nocodazole and taxol on the inhibitory and excitatory synaptic currents (the upward and downward deflections in current traces, respectively) and synaptic drives, which represent a correlate of respiratory motor activity.

participate in the mechanisms of neuronal plasticity which require spatiotemporal integration of long-term changes in $[Ca^{2+}]_i$.

In conclusion, the intrinsic motility of ER vesicles make them, together with mitochondria, optimally suited to dynamically adjust a local handling of $[Ca^{2+}]_i$ in neurons at such strategic 'hot spots' as synapses. Both organelles are transported along microtubules by the molecular motors of the kinesin family (Bannai et al., 2004). Modulation of their traffic in the regions of intense neuronal activity (Mironov, 2006) would increase the probability for mitochondria and ER vesicles to meet and act in a choreographed interplay, shaping the Ca^{2+} signals in neural processes. The mechanisms that are responsible for the targeted delivery, positioning and maintenance of the contacts between ER and mitochondria have to be elucidated. Similar to mitochondria (Stowers et al., 2002; Guo et al., 2005; Verstreken et al., 2005), there might be specific proteins that mediate the transport and anchoring of ER vesicles in the vicinity of synapses (Skehel et al., 2000).

Materials and Methods

Cell preparations and solutions

Cultured respiratory neurons were obtained from neonatal mice (NMRI, P3-P6) as described previously (Mironov et al., 2005b; Mironov, 2006). During the experiments, the coverslips with cells were mounted in the recording chamber which was continuously superfused at 34°C with artificial cerebrospinal fluid (ACSF) that contained 136 mM NaCl, 5 mM KCl, 1.25 mM $CaCl_2$, 0.8 mM $MgSO_4$, 0.4 mM NaH_2PO_4, 0.3 mM K_2HPO_4, 3.3 mM $NaHCO_3$ and 6 mM glucose, pH 7.4, and was saturated with 95% O_2-5% CO_2. All dyes were from Molecular Probes (MoBiTec, Göttingen, Germany) and all other chemicals were from Sigma (Deisenhofen, Germany). The drugs were either applied to the bath or were locally applied to the neural processes that within <0.1 seconds produced a 5 μm-wide spot of new solution (Mironov, 2006). Medullary slices containing a functional respiratory network (Smith et al., 1991) were obtained from neonatal mice as described previously (Mironov et al., 1998). Respiratory motor output was monitored extracellularly by applying a suction electrode to the hypoglossal (XII) nerve rootlets and the cells were voltage-clamped in the perforated patch mode (Mironov and Langohr, 2005).

Imaging

To characterise ER in the cultured respiratory neurons in terms of Ca^{2+} signalling, we used a 'lumenal Ca^{2+} monitoring technique' (Bannai et al., 2004). Neurons were loaded with a low-affinity (K_d=25 μM) fluorescent Ca^{2+} indicator dye Mag-Fura-2/AM (20 μM for 60 minutes in culture medium at 37°C) that was followed by incubation for 30 minutes in fresh medium to allow complete de-esterification of precursor dye. Residual indicator was washed out of the cytoplasm after brief membrane permeabilisation at 4°C with 10 μM β-escin for 90 seconds in a Ca^{2+}-free ASCF with 0.1 mM ethyleneglycotetraacetic acid (EGTA) and 3 mM adenosine 5′-triphosphate (ATP) added. The cells were subsequently washed with a cold (4°C) ACSF and were transferred into an experimental chamber in which the temperature was slowly raised to 34°C. Membrane depolarisations produced opposing changes in the fluorescence excited at 350 nm and 380 nm that reflected a Ca^{2+}-sensitivity of Mag-Fura-2 (Ukhanov et al., 1995). The ratio of fluorescence signals at 350 nm/380 nm was close to 0.5 at rest and increased to approximately 1 after the application of high-K^+ solutions. We also correlated ER patterns as revealed by Mag-Fura-2 with the distribution of EYFP-calreticulin (Clontech, Mountain View, CA) that was expressed in respiratory neurons as described previously (Mironov et al., 2005b). Mitochondria were stained with Rhod-2 by using the time-protocol of Mag-Fura-2 loading. Thapsigargin released Ca^{2+} only from Mag-Fura-2 but not from Rhod-2-stained organelles (n=6). Conversely, CCCP released Ca^{2+} only from Rhod-2 but not from Mag-Fura-2-stained organelles (n=5).

To image mitochondrial potential, we used TMRE (100 nM) and cells were equilibrated with the dye for 20 minutes. The synaptic vesicles were visualised with FM 1-43 (Betz et al., 1996). Neurons were stained with 8 μM FM 1-43 which was applied in the presence of 60 mM KCl for 60-120 seconds, and the cells were washed with a fresh ASCF for 5-10 minutes. Brief membrane depolarisations produced abrupt decreases in the fluorescence of FM 1-43, indicating the exocytosis of synaptic vesicles.

Fluorescence measurements were performed by using either a two-photon scanning microscope (TPSM) or a cooled CCD camera (MicroMax, Princeton Instruments, NJ) as described (Mironov et al., 2005b; Müller et al., 2005; Mironov, 2006). Both setups were based on the Zeiss Axioscope and they were routinely tested to confirm the absence of mechanical artefacts. TPSM was used in all experiments with a single indicator dye. Illumination wavelength was set to 760 nm (Mag-Fura-2) or 800 nm (YFP) and the pixel acquisition time was 7 μs. A CCD camera was used in the experiments with two indicator dyes. The emission was collected by using a dichroic mirror (510 mid-reflection) and the emission filters centered at 535±15 nm or 560±20 nm. The dyes were excited at 350 nm and 380 nm (Mag-Fura-2 and Fura-2), 460 nm (FM 1-43), and 490 nm (EYFP-calreticulin, Rhod-2, TMRE). The emission was filtered at 535 nm (Mag-Fura-2, Fura-2, EYFP and FM 1-43) or 560 nm (Rhod-2 and TMRE). Exposure times ranged from 100 to 300 ms and the frames were collected every 1 to 15 seconds. For offline analysis, the images were first deconvoluted and this improved the radial full-width-half-maximum (FWHM) from 0.9 to 0.3 μm (TPSM) and from 2.2 to 0.7 μm (CCD camera), which allowed for reliable recognition of submicron cytoplasmic particles at separations ⩾0.5 μm. The movies illustrating the movements of ER vesicles, their spatiotemporal relation to exocytosis and interactions with mitochondria are presented in the supplementary material.

Statistics

Changes in fluorescence of TMRE, Rhod-2 and FM 1-43 were measured in the regions of interest (ROI) that contained the fluorescence spots marked ER vesicles, mitochondria or synapses. The data are presented in per cent (ΔF) relative to the initial signal (F_0). Each test was repeated for at least five neurons from three different cell preparations. Data are represented as mean ± s.d. and the number of trials (n) is given. When required, the significance was also verified in unpaired two-tailed t-tests, comparing the mean of the observed changes with untreated control cells. The significance levels are given as P values (0.05 or 0.01).

We thank N. Hartelt for excellent technical assistance, and M. Müller and J. Schmidt for their help with a two-photon microscope.

References

Arnaudeau, S., Kelley, W. L., Walsh, J. V. and Demaurex, N. (2001). Mitochondria recycle Ca^{2+} to the endoplasmic reticulum and prevent the depletion of neighboring endoplasmic reticulum regions. *J. Biol. Chem.* **276**, 29430-29439.

Bannai, H., Inoue, T., Nakayama, T., Hattori, M. and Mikoshiba, K. (2004). Kinesin dependent, rapid, bi-directional transport of ER sub-compartment in dendrites of hippocampal neurons. *J. Cell Sci.* **117**, 163-175.

Baumann, O. and Walz, B. (2001). Endoplasmic reticulum of animal cells and its organization into structural and functional domains. *Int. Rev. Cytol.* **205**, 149-214.

Belair, E. L., Vallee, J. and Robitaille, R. (2005). Long-term in vivo modulation of synaptic efficacy at the neuromuscular junction of Rana pipiens frogs. *J. Physiol.* **569**, 163-178.

Bereiter-Hahn, J. and Voth, M. (1994). Dynamics of mitochondria in living cells: shape changes, dislocations, fusion, and fission of mitochondria. *Microsc. Res. Tech.* **27**, 198-219.

Berridge, M. J. (2002). The endoplasmic reticulum: a multifunctional signaling organelle. *Cell Calcium* **32**, 235-249.

Betz, W. J., Mao, F. and Smith, C. B. (1996). Imaging exocytosis and endocytosis. *Curr. Opin. Neurobiol.* **6**, 365-371.

Billups, B. and Forsythe, I. D. (2002). Presynaptic mitochondrial calcium sequestration influences transmission at mammalian central synapses. *J. Neurosci.* **22**, 5840-5847.

Brough, D., Schell, M. J. and Irvine, R. F. (2005). Agonist-induced regulation of mitochondrial and endoplasmic reticulum motility. *Biochem. J.* **392**, 291-297.

Brown, M. R., Sullivan, P. G. and Geddes, J. W. (2006). Synaptic mitochondria are more susceptible to Ca^{2+} overload than non-synaptic mitochondria. *J. Biol. Chem.* **281**, 11658-11668.

Carre, M., Andre, N., Carles, G., Borghi, H., Brichese, L., Briand, C. and Braguer, D. (2002). Tubulin is an inherent component of mitochondrial membranes that interacts with the voltage-dependent anion channel. *J. Biol. Chem.* **277**, 33664-33669.

Collins, T. J., Berridge, M. J., Lipp, P. and Bootman, M. D. (2002). Mitochondria are morphologically and functionally heterogeneous within cells. *EMBO J.* **21**, 1616-1627.

Evtodienko, Y. V., Teplova, V. V., Sidash, S. S., Ichas, F. and Mazat, J. P. (1996). Microtubule-active drugs suppress the closure of the permeability transition pore in tumour mitochondria. *FEBS Lett.* **393**, 86-88.

Guo, X. G., Macleod, T., Wellington, A., Hu, F., Panchumarthi, S., Schoenfield, M., Marin, L., Charlton, M. P., Atwood, H. L. and Zinsmaier, K. E. (2005). The GTPase dMiro is required for axonal transport of mitochondria to Drosophila synapses. *Neuron* **47**, 379-393.

Ichas, F. and Mazat, J. P. (1998). From calcium signaling to cell death: two conformations for the mitochondrial permeability transition pore. Switching from low- to high-conductance state. *Biochim. Biophys. Acta* **1366**, 33-50.

Ishii, K., Hirose, K. and Iino, M. (2006). Ca^{2+} shuttling between endoplasmic reticulum and mitochondria underlying Ca^{2+} oscillations. *EMBO Rep.* **7**, 390-396.

Kampa, B. M., Letzkus, J. J. and Stuart, G. J. (2006). Requirement of dendritic calcium spikes for induction of spike-timing-dependent synaptic plasticity. *J. Physiol.* **574**, 283-290.

Kidd, J. F., Pilkington, M. F., Schell, M. J., Fogarty, K. E., Skepper, J. N., Taylor, C. W. and Thorn, P. (2002). Paclitaxel affects cytosolic calcium signals by opening the mitochondrial permeability transition pore. *J. Biol. Chem.* **277**, 6504-6510.

Koshiya, N. and Smith, J. C. (1999). Neuronal pacemaker for breathing visualized in vitro. *Nature* **400**, 360-363.

Malli, R., Frieden, M., Osibow, K., Zoratti, C., Mayer, M., Demaurex, N. and Graier, W. F. (2003). Sustained Ca^{2+} transfer across mitochondria is essential for mitochondrial Ca^{2+} buffering, store-operated Ca^{2+} entry, and Ca^{2+} store refilling. *J. Biol. Chem.* **278**, 44769-44779.

Markram, H., Helm, P. J. and Sakmann, B. (1995). Dendritic calcium transients evoked by single back-propagating action potentials in rat neocortical pyramidal neurons. *J. Physiol.* **485**, 1-20.

Medler, K. and Gleason, E. L. (2002). Mitochondrial Ca^{2+} buffering regulates synaptic transmission between retinal amacrine cells. *J. Neurophysiol.* **87**, 1426-1439.

Mironov, S. L. (2006). Spontaneous and evoked neuronal activities regulate movements of single neuronal mitochondria. *Synapse* **59**, 403-411.

Mironov, S. L. and Richter, D. W. (2001). Oscillations and hypoxic changes of mitochondrial variables in neurons of the brainstem respiratory centre. *J. Physiol.* **533**, 227-236.

Mironov, S. L. and Langohr, K. (2005). Mechanisms of Na^{+} and Ca^{2+} influx into respiratory neurons during hypoxia. *Neuropharmacology* **48**, 1056-1065.

Mironov, S. L., Langohr, K., Haller, M. and Richter, D. W. (1998). Hypoxia activates ATP-dependent potassium channels in inspiratory neurones of neonatal mice. *J. Physiol.* **509**, 755-766.

Mironov, S. L., Hartelt, N. and Ivannikov, M. V. (2005a). Mitochondrial K(ATP) channels in respiratory neurons and their role in the hypoxic facilitation of rhythmic activity. *Brain Res.* **1033**, 20-27.

Mironov, S. L., Ivannikov, M. V. and Johansson, M. (2005b). $[Ca^{2+}]_i$ signalling between mitochondria and endoplasmic reticulum in neurons is controlled by microtubules: from mPTP to CICR. *J. Biol. Chem.* **280**, 715-721.

Müller, M., Mironov, S. L., Ivannikov, M. V., Schmidt, J. and Richter, D. W. (2005). Mitochondrial organization and motility probed by two-photon microscopy in cultured mouse brainstem neurons. *Exp. Cell Res.* **303**, 114-127.

Miyata, M., Finch, E. A., Khiroug, L., Hashimoto, K., Hayasaka, S., Oda, S. I., Inouye, M., Takagishi, Y., Nishiyama, M., Hong, K. et al. (2000). Calcium stores regulate the polarity and input specificity of synaptic modification. *Nature* **408**, 584-588.

Pivovarova, N. B., Pozzo-Miller, L. D., Hongpaisan, J. and Andrews, S. B. (2002). Correlated calcium uptake and release by mitochondria and endoplasmic reticulum of CA3 hippocampal dendrites after afferent synaptic stimulation. *J. Neurosci.* **22**, 10653-10661.

Reyes, M. and Stanton, P. K. (1996). Induction of hippocampal long-term depression requires release of Ca^{2+} from separate presynaptic and postsynaptic intracellular stores. *J. Neurosci.* **16**, 5951-5960.

Richter, D. W., Mironov, S. L., Büsselberg, D., Bischof, A. M., Lalley, P. M. and Wilken, B. (2000). Respiratory rhythm generation: plasticity of a neuronal network. *Neuroscientist* **6**, 188-205.

Rizzuto, R., Duchen, M. R. and Pozzan, T. (2004). Flirting in little space: the ER/mitochondria Ca^{2+} liaison. *Sci. STKE* **215**, Re1.

Saxton, M. J. and Jacobson, K. (1997). Single-particle tracking: applications to membrane dynamics. *Annu. Rev. Biophys. Biomol. Struct.* **26**, 373-399.

Shupliakov, O., Bloom, O., Gustafsson, J. S., Kjaerulff, O., Low, P., Tomilin, N., Pieribone, V. A., Greengard, P. and Brodin, L. (2002). Impaired recycling of synaptic vesicles after acute perturbation of the presynaptic actin cytoskeleton. *Proc. Natl. Acad. Sci. USA* **99**, 14476-14481.

Skehel, P. A., Fabian-Fine, R. and Kandel, E. R. (2000). Mouse VAP33 is associated with the endoplasmic reticulum and microtubules. *Proc. Natl. Acad. Sci. USA* **97**, 1101-1106.

Smith, J. C., Ellenberger, H. H., Ballanyi, K., Richter, D. W. and Feldman, J. L. (1991). Pre-Bötzinger complex: a brainstem region that may generate respiratory rhythm in mammals. *Science* **254**, 726-729.

Spacek, J. and Harris, K. M. (1997). Three-dimensional organization of smooth endoplasmic reticulum in hippocampal CA1 dendrites and dendritic spines of the immature and mature rat. *J. Neurosci.* **17**, 190-203.

Stowers, R. S., Megeath, L. J., Gorska-Andrzejak, J., Meinertzhagen, I. A. and Schwarz, T. L. (2002). Axonal transport of mitochondria to synapses depends on milton, a novel Drosophila protein. *Neuron* **36**, 1063-1077.

Takechi, H., Eilers, J. and Konnerth, A. (1998). A new class of synaptic response involving calcium release in dendritic spines. *Nature* **396**, 757-760.

Takei, K., Shin, R. M., Inoue, T., Kato, K. and Mikoshiba, K. (1998). Regulation of nerve growth mediated by inositol 1,4,5-trisphosphate receptors in growth cones. *Science* **282**, 1705-1708.

Terasaki, M., Slater, N. T., Fein, A., Schmidek, A. and Reese, T. S. (1994). Continuous network of endoplasmic reticulum in cerebellar Purkinje neurons. *Proc. Natl. Acad. Sci. USA* **91**, 7510-7514.

Ukhanov, K. Y., Flores, T. M., Hsiao, H. S., Mohapatra, P., Pitts, C. H. and Payne, R. (1995). Measurement of cytosolic Ca^{2+} concentration in Limulus ventral photoreceptors using fluorescent dyes. *J. Gen. Physiol.* **105**, 95-116.

Verstreken, P., Ly, C. V., Venken, K. J. T., Koh, T. W., Zhou, Y. and Bellen, H. J. (2005). Synaptic mitochondria are critical for mobilization of reserve pool vesicles at Drosophila neuromuscular junctions. *Neuron* **47**, 365-378.

Volpe, P., Villa, A., Damiani, E., Sharp, A. H., Podini, P., Snyder, S. H. and Meldolesi, J. (1991). Heterogeneity of microsomal Ca^{2+} stores in chicken Purkinje neurons. *EMBO J.* **10**, 3183-3189.

Waterman-Storer, C. M. and Salmon, E. D. (1998). Endoplasmic reticulum membrane tubules are distributed by microtubules in living cells using three distinct mechanisms. *Curr. Biol.* **8**, 798-806.

White, C., Li, C., Yang, J., Petrenko, N. B., Madesh, M., Thompson, C. B. and Foskett, J. K. (2005). The endoplasmic reticulum gateway to apoptosis by Bcl-X(L) modulation of the InsP3R. *Nat. Cell Biol.* **7**, 1021-1028.

Yi, M., Weaver, D. and Hajnoczky, G. (2004). Control of mitochondrial motility and distribution by the calcium signal: a homeostatic circuit. *J. Cell Biol.* **167**, 661-672.

Zucker, R. S. (1999). Calcium- and activity-dependent synaptic plasticity. *Curr. Opin. Neurobiol.* **9**, 305-313.